

Non-invasive Oil-Based Method to Increase Topical Delivery of Nucleic Acids to Skin

Manika Vij,^{1,4} Shamshad Alam,² Nidhi Gupta,³ Vishvabandhu Gotherwal,^{1,4} Hemlata Gautam,¹ Kausar M. Ansari,² Deenan Santhiya,³ Vivek T. Natarajan,^{1,4} and Munia Ganguli^{1,4}

¹CSIR-Institute of Genomics and Integrative Biology, South Campus, Mathura Road, New Delhi 110020, India; ²CSIR-Indian Institute of Toxicology Research, Post Box 80, Mahatma Gandhi Marg, Lucknow (Uttar Pradesh) 226001, India; ³Delhi Technological University, Shahbad Daulatpur, Main Bawana Road, New Delhi 110042, India; ⁴Academy of Scientific and Innovative Research (AcSIR), Anusandhan Bhawan, 2 Rafi Marg, New Delhi 110001, India

Topical delivery of nucleic acids to skin has huge prospects in developing therapeutic interventions for cutaneous disorders. In spite of initial success, clinical translation is vastly impeded by the constraints of bioavailability as well as stability in metabolically active environment of skin. Various physical and chemical methods used to overcome these limitations involve invasive procedures or compounds that compromise skin integrity. Hence, there is an increasing demand for developing safe skin penetration enhancers for efficient nucleic acid delivery to skin. Here, we demonstrate that pretreatment of skin with silicone oil can increase the transfection efficiency of non-covalently associated peptide-plasmid DNA nanocomplexes in skin ex vivo and in vivo. The method does not compromise skin integrity, as indicated by microscopic evaluation of cellular differentiation, tissue architecture, enzyme activity assessment, dye penetration tests using Franz assay, and cytotoxicity and immunogenicity analyses. Stability of nanocomplexes is not hampered on pretreatment, thereby avoiding nuclease-mediated degradation. The mechanistic insights through Fourier transform infrared (FTIR) spectroscopy reveal some alterations in the skin hydration status owing to possible occlusion effects of the enhancer. Overall, we describe a topical, non-invasive, efficient, and safe method that can be used to increase the penetration and delivery of plasmid DNA to skin for possible therapeutic applications.

INTRODUCTION

Recent developments in topical and transdermal delivery across skin highlight its immense potential for administration of therapeutics as well as cosmeceutics.^{1–3} In addition to the advantages of large surface area and easy access, therapeutic delivery through skin can also bypass the hepatic metabolism of oral delivery.^{4,5} Although a wide repertoire of cargo has been delivered in skin, the clinical benefits achieved are still limited.^{6,7} This limitation is largely attributed to the poor percutaneous permeability of administered cargo molecules owing to the significant barrier properties of skin. The major barrier is imposed by its superficial layer, the stratum corneum, whose unique lipid-rich composition along with richness of desmosomes effectively impedes the entry of hydrophilic macromolecules.^{5,8} Moreover the delivered molecules should also enter skin in therapeutically sufficient

amounts in order to efficaciously alleviate the condition without disturbing the skin integrity. In order to achieve this, researchers have focused on different strategies based on physical interventions or chemical and carrier-based methods.^{9–15} However, many of these methods suffer from an invasive nature, cumbersome application, and toxic effects, which render them noncompliant for practical use.^{11,16}

Synthetic and essential oils constitute a category of enhancers being explored for improved delivery to skin in a nontoxic manner. Polysiloxane or silicone oil (polymerized siloxane with organic side chains) is used as a component in many of these enhancers. Silicone oil has many applications determined by its structure, viscosity, volatile nature, and thermal stability. In skin care, silicones (oil or variants) have been used to prepare sunscreen formulations, non-sticky moisturizers, and body perspirants. It also has therapeutic applications, such as facilitating collagen production in hypertrophic scars and providing sealant properties in wound-healing applications to avoid subsequent invasion by pathogens.^{17–20} In spite of large-scale applications in skin with limited or no safety concerns, it has still not been explored much as a skin penetration enhancer for increased delivery of macromolecules.

Recently, skin-penetrating peptides (SPPs) have also emerged as relatively safe and non-invasive agents that assist efficient entry of both small and macromolecules across skin either through co-administration or non-covalent association.^{21–29} Therefore, it is interesting to explore whether they can serve as potential alternatives to the existing chemical penetration enhancers. Insights will help us not only design better penetration enhancers with minimal side effects but also realize its therapeutic benefit in clinical settings. Most of these methods mentioned above are able to mediate increased entry of molecules in skin by means of interaction with skin lipids or proteins, leading to reversible alterations in skin permeability.^{11,16}

Received 7 June 2016; accepted 8 March 2017;
<http://dx.doi.org/10.1016/j.ymthe.2017.03.009>.

Correspondence: Munia Ganguli, CSIR-Institute of Genomics and Integrative Biology, South Campus, Room No. 225/Lab No. 219, Mathura Road, New Delhi 110020, India.

E-mail: mganguli@igib.res.in

In the present work, we used silicone oil, a chemical enhancer, and a peptide enhancer and analyzed if they were able to improve plasmid DNA delivery efficiency to skin *ex vivo* and *in vivo* in a synergistic manner. We applied these chemicals as pretreatments before delivering plasmid DNA as a nanocomplex with a SPP, Mgpe9, which was developed earlier in our laboratory.³⁰ We evaluated the safety potential of these enhancers at both the tissue and cellular levels using fluorescence microscopy, skin integrity assessment, and cytotoxicity and immunogenicity analyses. We propose that silicone oil is an efficient penetration enhancer for improved plasmid DNA delivery to skin with minimal side effects. For a better understanding of its interaction with skin, we also tried to elucidate the mechanism by which silicone oil achieves its desired action on skin. Overall, we report an effective and safe strategy for enhancing bioavailability of peptide-plasmid DNA nanocomplexes in skin using silicone oil.

RESULTS

We planned our study using two chemical enhancers (sodium laureth sulfate-phenyl piperazine [SLA-PP] and silicone oil) and a SPP enhancer (TD-1) that have been previously used for enhancing delivery of small molecules, but not nanocomplexes.^{9,23,31} Initially, we studied the effects of their pre-application on transfection efficiency and skin integrity followed by possible mechanisms of action.

Silicone Oil Enhanced EGFP Expression in Skin *Ex Vivo*, *In Vivo*, and *In Vitro* without Altering Nanocomplex Stability

We first explored the effect of different enhancers on stability of the nanocomplexes. The complexes were prepared at charge ratio 10 to ensure small particle size, positive surface charge, and little or no aggregation through charge-charge repulsion, thereby maintaining colloidal stability. This has already been standardized and reported by us in a previous study.³⁰ To check the stability of these nanocomplexes, we first estimated their size in the presence of enhancers using dynamic light scattering and then performed a DNA condensation assay in which the integrity of the nanocomplex could be determined. Although we observed an overall increase in the size of the nanocomplexes in the presence of all the enhancers (Figure 1A), the complex integrity remained unaffected in the presence of silicone oil and TD-1 as seen by absence of free plasmid DNA in the gel image (Figure 1B), unlike in the case of SLA-PP, where plasmid DNA release along with some degradation was evident.

We then tested the ability of these enhancers to improve the entry of Mgpe9-pDNA nanocomplexes in skin. To study this, human skin tissue was topically pretreated with each of these enhancers *ex vivo*, followed by administration of nanocomplex using an application regimen standardized and described in our previous study (see [Materials and Methods](#) for further details).³⁰ The enhancement effect was monitored by checking for increase in transfection efficiency of Mgpe9 nanocomplexes. Both qualitative (Figure 1C) and quantitative (Figures 1D and S1) estimation of EGFP-C1 fluorescence in skin showed that silicone oil achieved maximum increase in EGFP expression. While the basal level of ~30% fluorescence-positive cells was obtained using only the Mgpe9-pDNA nanocomplexes, >45% fluo-

rescence-positive cells and high mean intensity were observed in the presence of silicone oil. The transfection efficiency with application of SLA-PP was slightly less (i.e., ~40% fluorescence-positive cells with low mean intensity) than that observed with silicone oil. Moreover, the microscopic investigation shown in Figure 1C indicated some loss of skin architecture upon treatment with SLA-PP, which we explore and discuss later in the text. TD-1 did not seem to produce any obvious changes in skin architecture but gave negligible fluorescence upon qualitative estimation and fewer fluorescence-positive cells with very low mean intensity.

Owing to its maximum enhancement efficiency *ex vivo*, we went on to explore the utility of silicone oil as an enhancer under *in vivo* conditions using hairless mouse SKH-1 as a model organism. It was observed that pretreatment with silicone oil increased the percentage of EGFP-positive cells obtained by ~10% in comparison to the condition when only Mgpe9 nanocomplexes were applied (Figures 1E and S2A). Moreover, luciferase transfection efficiency in the SKH-1 mouse also exhibited one order increase in expression upon silicone oil pretreatment (Figure S2B). Thus, irrespective of the different nature of two skin types (*ex vivo* and *in vivo*), silicone oil increased the efficiency of delivery in both. Moreover, a similar trend of expression was observed in human primary keratinocytes *in vitro* (Figure S3). However, SLA-PP was unable to give similar expression owing to its toxic effect on cells (Figure S3). Since these chemical enhancers and SPP also have the propensity to enter skin by themselves, we next analyzed whether their application caused any adverse effects on skin.

Silicone Oil Did Not Show Any Toxic Effects on *Ex Vivo*, *In Vivo*, and *In Vitro* Administration in Human Skin or SKH-1

One of the major concerns about use of enhancer molecules in skin is their safety potential. So we next carried out a detailed toxicity assessment of silicone oil and SLA-PP, at both tissue and cellular levels. Since TD-1 was not efficient in enhancing the EGFP signal, it was excluded from further experiments. Any possible change in tissue architecture on enhancer treatment was studied using confocal microscopy. In particular, cellular differentiation and disruption of the barrier layer of stratum corneum was monitored by checking the presence or absence of keratin 10, loricrin, and keratin 14 markers in the different layers of skin. It was observed visually that the stratum corneum did not become dissociated upon silicone oil pretreatment followed by topical administration of Mgpe9 nanocomplexes, unlike with SLA-PP, where it was completely dismantled (Figure 2A). Moreover, the presence of keratin 10, loricrin, and keratin 14 marker proteins in the different layers of skin was clearly evident with bare silicone oil treatment contrary to bare SLA-PP treatment, where the keratin 14 signal was completely lost from the skin tissue and loricrin or keratin 10 layers were completely distorted (Figures 2B and S4).

Further, we also performed a skin integrity assessment using a dye penetration test (using low-molecular-weight fluorescein isothiocyanate [FITC] and high-molecular-weight dextran) across skin in order to assess the adverse effect, if any, at the tissue level (Figures 2C and

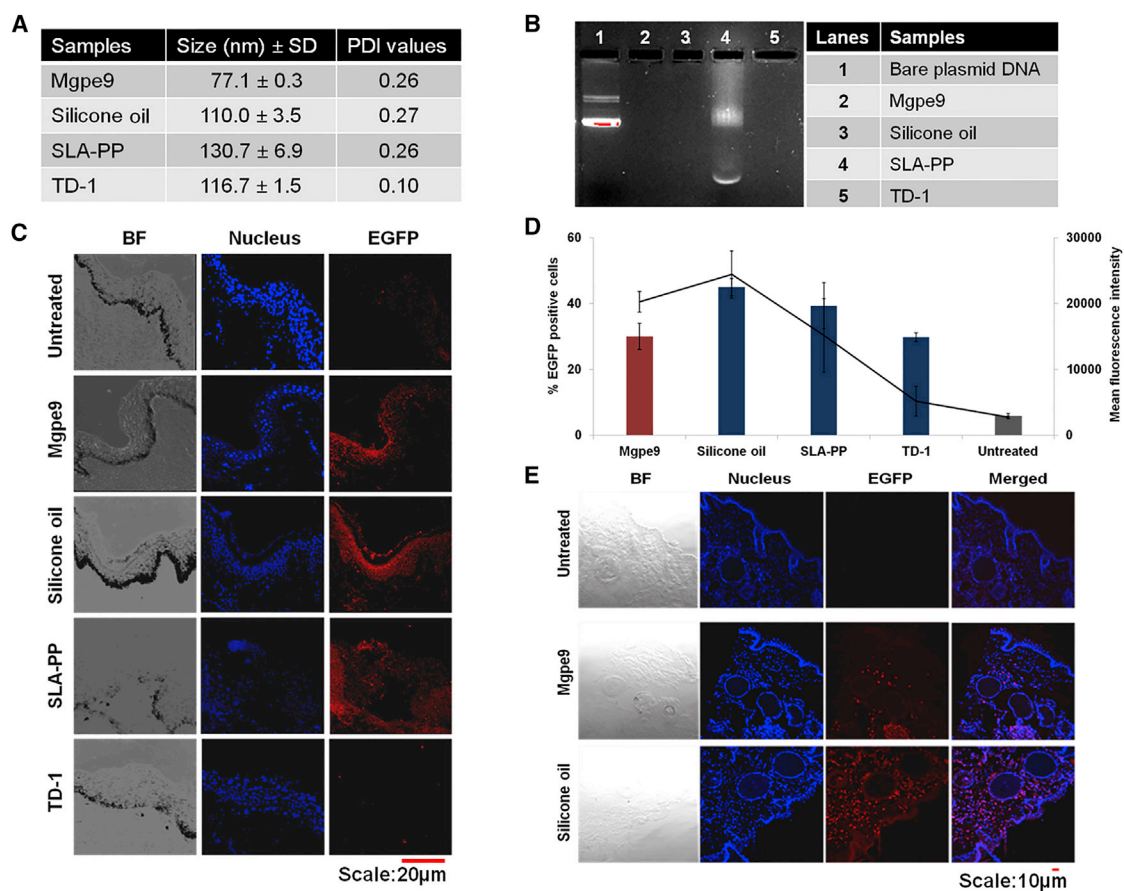


Figure 1. Effect of Skin Penetration Enhancers on Biophysical Characteristics and Ex Vivo and In Vivo Transfection Efficiency of Mgpe9 Nanocomplexes

(A) Size estimation of Mgpe9 nanocomplexes, native or in the presence of enhancers (i.e., silicone oil, SLA-PP, and TD-1), where hydrodynamic diameter was measured using dynamic light scattering. Data are presented as size \pm SD. PDI, poly-dispersity index. (B) DNA condensation assay was performed to check the stability of Mgpe9 nanocomplexes, either native or in the presence of different enhancers as mentioned in Figure 1A. Stability was assessed visually on 1% agarose gel as the amount of plasmid DNA released upon electrophoresis in comparison to the control plasmid DNA loaded in lane 1. Ethidium bromide was used to impart fluorescence and detect presence of free plasmid DNA in gel. (C) Visualization of increase in EGFP expression in human skin tissue (ex vivo) using confocal microscopy upon enhancer pretreatment. Skin tissue was topically pretreated with enhancers, followed by subsequent administration of Mgpe9 nanocomplexes (one application per day with 4 μ g plasmid DNA per application) for three consecutive days (as detailed in Materials and Methods). Immunostaining was carried out using the protocol detailed in Materials and Methods (to avoid auto-fluorescence artifact), and confocal imaging was performed at 40 \times magnification. TRITC (red) indicates EGFP expression, and DAPI (blue) was used as a nuclear stain to show epidermal cell viability. Scale bar, 20 μ m. (D) Quantitative analysis of EGFP expression in human skin tissue (ex vivo) was carried out using flow cytometry. The percentage of EGFP-positive cells (bar graph) and the mean fluorescence intensity (line graph) were recorded. The data are shown as mean \pm SD; $p < 0.001$ was observed for silicone oil, where $n = 6$ (triplicates). The red bar indicates Mgpe9 nanocomplex, the blue bar indicates enhancers + Mgpe9 nanocomplex, and the gray bar indicates control (no treatment). (E) In vivo enhancement of transfection efficiency for Mgpe9 nanocomplexes in SKH-1 mice was assessed using confocal microscopy as detailed in Materials and Methods. EGFP expression was assessed through immunostaining, and imaging was done at 20 \times magnification. TRITC (red) indicates EGFP expression, and DAPI (blue) was used as a nuclear stain to show epidermal cell viability. Scale bar, 10 μ m. See also Figures S1–S3.

S5A). Any recordable presence of these dyes in the receptor solution of Franz apparatus on co-administration with enhancer and Mgpe9 nanocomplexes would indicate compromised skin tissue integrity. We observed that silicone oil did not allow dye penetration, indicating uncompromised skin integrity and the absence of tissue damage, unlike what was observed with SLA-PP. However, we also did not detect the presence of FITC fluorescence in the skin tissue upon microscopic examination, indicating no permeation of dye (Figure S5B); the possible reason for this has been elaborated in the Discussion.

We next monitored the change in protease activity in skin to see if there was any effect on the active metabolic environment as a result of these treatments. We observed that silicone oil along with treatment with Mgpe9 nanocomplexes did not show any major change in protease activity, unlike with SLA-PP, where significant loss of protease activity (>60% loss) was recorded (Figure 2D). Further, we wanted to explore whether silicone oil had any adverse effects on the viable cells in epidermis under similar conditions, for which we used propidium iodide staining and checked for cell death in skin tissue (Figure 2E). Silicone oil did not exhibit any toxic effects, as

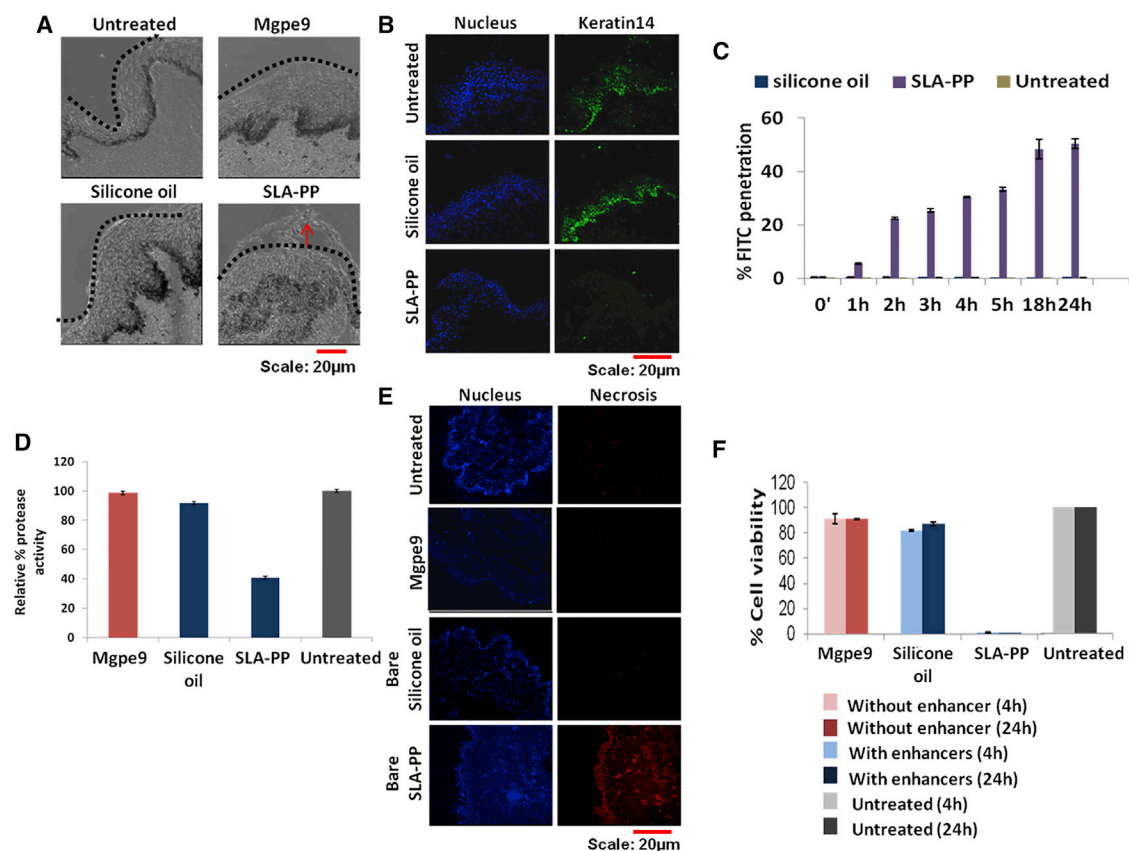


Figure 2. Safety Evaluation of Silicone Oil as an Enhancer in Skin in the Presence of Mgpe9 Nanocomplexes

(A) The synergistic effect of silicone oil enhancer and Mgpe9 nanocomplexes on stratum corneum barrier of skin was observed using confocal microscopy. Imaging of human skin cryosections (6 μm) was performed at 40 \times magnification to visually locate detachment or complete abolishment of the stratum corneum upon topical treatment administration. SLA-PP was used for comparison. Scale bar, 20 μm . (B) The effect of bare silicone oil and SLA-PP applications on skin tissue architecture was studied using immunostaining to highlight the presence of keratin 14 protein, which is a known biochemical marker for the basal layer of skin. The green signal of Alexa 488 indicates the basal layer of skin; DAPI dye (blue) was used to stain the nuclei of viable epidermal cells. Untreated skin tissue was used as an experimental control. Complete absence of green fluorescence indicates damage to the basal layer of skin. Scale bar, 20 μm . (C) Skin integrity on application of silicone oil/SLA-PP and Mgpe9 nanocomplexes was assessed by a dye-penetration test using the Franz diffusion assay. SLA-PP was used as a positive control for this study. Penetration of the low-molecular-weight dye FITC was studied. Data are shown as mean \pm SD. (D) Non-specific protease activity in human skin tissue (pretreated with enhancers and nanocomplexes) was estimated by standard BCA using casein as the substrate. Tyrosine (1 mg/mL) was used to plot the standard curve. Enzymatic activity obtained from untreated skin tissue was taken as 100%, and relative percentage of enzyme activity was plotted for treatments. The red bar indicates Mgpe9 nanocomplex, the blue bar indicates enhancers + Mgpe9 nanocomplex, and the gray bar indicates control (no treatment). (E) Fluorescence microscopy analysis was performed on treated human skin on application of silicone oil/SLA-PP and Mgpe9 nanocomplexes to check for necrotic cell death in viable epidermis using the propidium iodide dye staining method. Dead cells were identified by presence of red fluorescence. Images were obtained at 20 \times magnification. Scale bar, 20 μm . (F) Cell viability in presence of enhancers and Mgpe9 nanocomplexes was assessed using CellTiter Glo Luminescent Cell Viability assay for 4 hr and 24 hr in HaCaT cells. Bare nanocomplex treatment was performed for comparative analysis. Untreated cells were considered as 100% viable. Values were plotted as relative percentage of cell viability for all the treatments. Data are shown as mean \pm SD. The red bar indicates Mgpe9 nanocomplex, the blue bar indicates enhancers + Mgpe9 nanocomplex, and the gray bar indicates control (no treatment). See also Figures S4–S7.

evidenced by the absence of red fluorescence in the skin tissue, whereas SLA-PP seemed to be highly toxic. To confirm our observation, we also performed a cytotoxicity assessment on HaCaT (human adult keratinocyte) cells as well as human primary keratinocytes under in vitro conditions (to mimic transfection application) and observed a similar trend (Figures 2F and S6). More than 80% cell viability was maintained in the presence of silicone oil, as compared to SLA-PP, where merely 10% cells survived upon exposure to the enhancer at 24 hr in both the cell lines. We further checked the serum

for the presence of inflammatory cytokines such as interleukin 2 (IL-2), IL-6, IL-12, and tumor necrosis factor alpha (TNF- α) on application of enhancers as well as nanocomplexes on SKH-1 mice in vivo. However, we did not observe a significant upregulation of any of these inflammatory cytokines in the presence of silicone oil, unlike SLA-PP (Figure S7). All of these observations cumulatively indicated that silicone oil was the best enhancer for plasmid DNA delivery among the ones we studied. Therefore, we next attempted to understand its mechanism of action on skin.

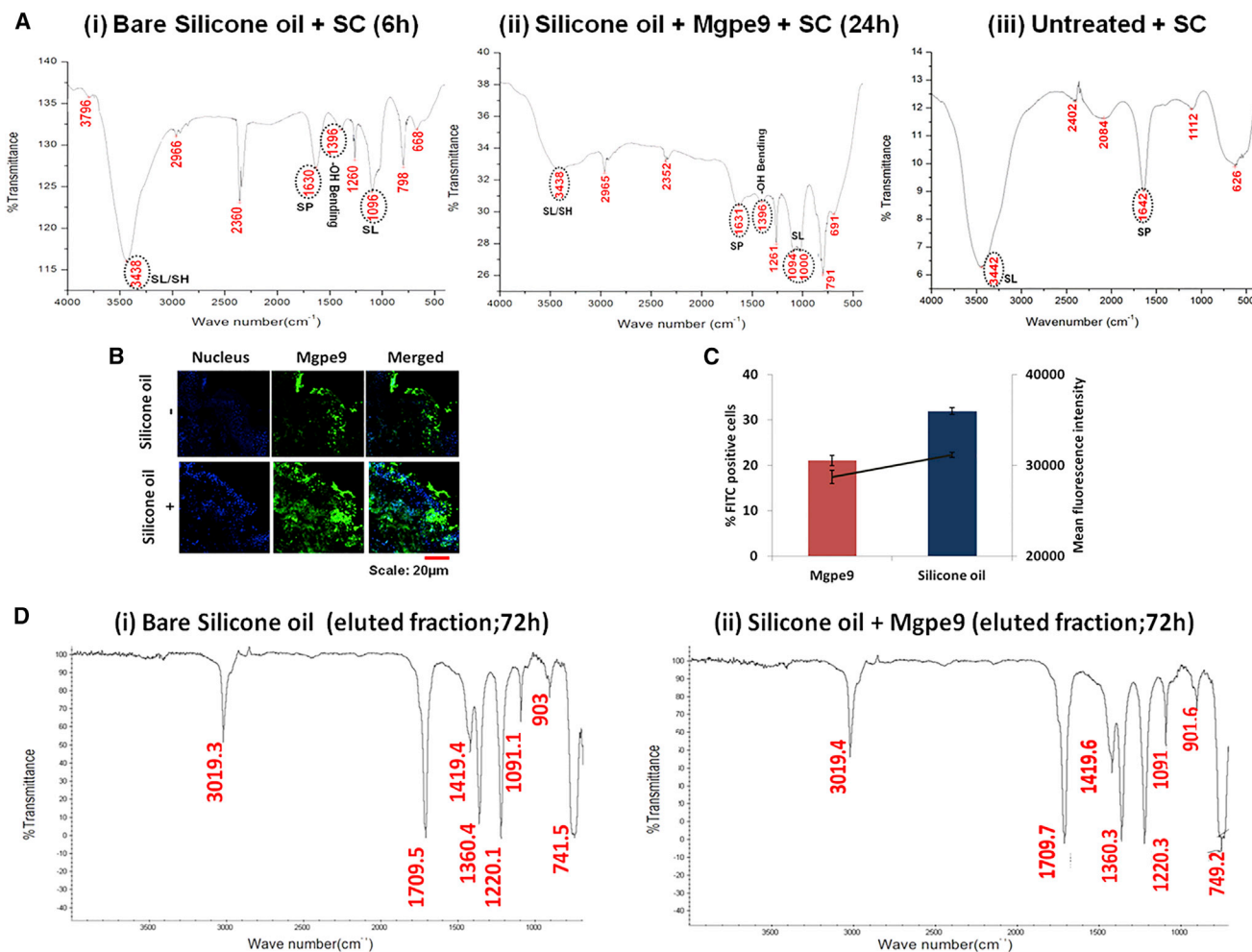


Figure 3. Mechanistic Insights into Enhancement Effects of Silicone Oil upon Topical Treatment in Skin

(A) FTIR spectroscopy was carried out on the stratum corneum of human skin treated with silicone oil and Mgpe9 nanocomplexes (as a single topical application) for 24 hr (ii) to predict interaction with skin components. Untreated stratum corneum (i) was used as an experimental control. Critical peaks are indicated in red circles. SL, skin lipids; SP, skin proteins; SH, skin hydration; LF/LE, lipid fluidization/lipid extraction; PI, protein interaction. (B) Tissue uptake of labeled Mgpe9 nanocomplexes (formed using FITC-labeled plasmid DNA and unlabeled peptide) in the presence and absence of silicone oil enhancer was studied using confocal microscopy. Cells were imaged at 40 \times magnification to demonstrate the entry of nanocomplexes across stratum corneum and into the viable epidermal cells of skin. Scale bar, 20 μ m. (C) Quantitative estimation of tissue uptake of labeled Mgpe9 nanocomplexes in the presence and absence of silicone oil enhancer was carried out using flow cytometry. The percentage of FITC-positive cells (bar graph) and the mean fluorescence intensity (line graph) were recorded. Data are shown as mean \pm SD. The red bar indicates Mgpe9 nanocomplex, and the blue bar indicates enhancers + Mgpe9 nanocomplex. (D) To check silicone oil entry in skin, FTIR spectroscopy was performed on a chloroform/acetone elute solution obtained from viable epidermis of tape-stripped human skin tissue pretreated with (i) bare silicone oil or (ii) silicone oil and Mgpe9 nanocomplexes as three consecutive topical administrations. All peaks are indicated in red. See also Figure S8.

Silicone Oil Enhanced the Entry of Nanocomplexes, Possibly through Occlusive Effects

Silicone oil is well known for its occlusive effects as well as capturing of nanoparticles on skin. Hence, we wanted to explore if, in this case, it allowed longer retention of the nanocomplexes in skin, directed the higher entry in skin through increasing the skin hydration pressure, or induced major structural alterations of the skin. Fourier transform infrared (FTIR) spectroscopy was carried out on the stratum corneum of human skin^{10,16,32–35} treated with silicone oil and Mgpe9 nano-

complexes for 24 hr (to mimic an actual one-time application) (Figure 3A). Untreated skin was considered as the experimental control. In the case of the untreated stratum corneum, we observed a peak at 3,442 cm^{-1} , which could be attributed to the C-H asymmetric and symmetric stretching of the skin lipids, whose peaks are usually attributed from 2,800 to 2,950 cm^{-1} but are often merged with the broad peaks coming from the -OH stretching of water. Additionally, the presence of a 1,642 cm^{-1} peak in untreated tissue in our experiment indicated the presence of an amide I region of the skin proteins.^{10,34}

In case of the treated stratum corneum, the strongest peak was observed at $3,438\text{ cm}^{-1}$ and was much broader than that in the untreated sample, indicating either some mild structural alterations due to lipid extraction or fluidization or alteration in hydration status of skin (as inferred from the assignments described above). Moreover, the fluidity of the lipid and the changes in the nature of lipid packing can also be assessed by the bands in the region $1,000\text{--}1,400\text{ cm}^{-1}$, where we observed slight merging of the $1,094\text{ cm}^{-1}$ and $1,000\text{ cm}^{-1}$ peaks in 24-hr-treated sample. Another overlapping peak at $1,396\text{ cm}^{-1}$ seemed to be more evident in the treated sample, which could again be due to OH bending, indicating the probable presence of water molecules.

We also observed broadening of peak at $1,631\text{ cm}^{-1}$ in the treated sample, indicating alteration in protein structure. However, observation of tissue sample treated with only silicone oil (Figure S8A) did not show such a change, indicating that silicone oil is not responsible for this alteration of protein structure. The additional presence of nanocomplexes in the treated sample (Figure 3A) might suggest an interaction with skin proteins (as shown by us in our earlier report),³⁰ leading to alteration in this spectral region. Overall, no major alterations of skin structure seemed to be evident; however, mild lipid reorganization and changes in hydration status of skin seemed to be the primary observed changes and could be contributing to the enhancement of nanocomplex delivery instead of increased retention for mediating entry of nanocomplexes in skin.

In order to confirm this, we next checked the tissue uptake of FITC-labeled nanocomplexes in skin. We could observe an increase in FITC fluorescence across skin in the presence of silicone oil both qualitatively (Figure 3B) and quantitatively (Figure 3C) with an approximately >10% increase in the percentage of positive cells in the presence of the enhancer. This also helped us to rule out the possibility of longer retention of nanocomplexes on skin by silicone oil, where we would have expected less entry of complexes into the viable epidermis with higher localization on stratum corneum, unlike the observation in Figure 3B.

We next explored if silicone oil by itself entered skin by trying to retrieve it from viable epidermis of treated skin tissue (for a complete description of the application, see Materials and Methods). Stratum corneum was removed by tape-stripping, and silicone oil was eluted using a chloroform/acetone (1:1 v/v) mixture from viable epidermis. We compared the FTIR spectra of bare silicone oil and eluted fractions. Silicone oil is known to exhibit signature peaks at $1,260\text{ cm}^{-1}$ and $1,080\text{ cm}^{-1}$ denoting Si-CH₃ vibration and peak at $\sim 1,000\text{ cm}^{-1}$ or $\sim 700\text{ cm}^{-1}$ denoting Si-O vibration, respectively. We could observe presence of these peaks in the control sample (i.e., bare silicone oil) (Figure S8B), where peaks at $1,260\text{ cm}^{-1}$ and 753 cm^{-1} were present but peaks at $1,080\text{ cm}^{-1}$ and $1,000\text{ cm}^{-1}$ seemed to be merged to show a broad peak at $1,028\text{ cm}^{-1}$.^{32,33} However, the FTIR spectra of eluted fractions (Figure 3D) exhibited no traces of silicone oil peaks either in bare treatment or with nanocomplexes, indicating its absence from viable epidermis. Overall, this indi-

cated that silicone oil did not penetrate into deeper layers of skin and that its action is surface mediated. This would also rule out the risk of immunogenic effects upon its permeation beyond epidermis during in vivo delivery, as was also observed in previous section (Figure S7). However, this could also be attributed to solubility constraints of this enhancer and needs further validation.

DISCUSSION

The stratum corneum forms an effective barrier against movement of large hydrophilic molecules across skin, thereby allowing only small (<500 Da) lipophilic molecules to go through. Recent technological developments report many carriers that have the ability to penetrate stratum corneum but are unable to reach their designated sites in therapeutically sufficient amounts. Hence, their functional utility for both therapeutics and cosmeceuticals is vastly impeded by the unique architecture of the tissue. Many strategies have been devised to overcome this limitation and enhance the overall penetration of hydrophilic molecules, particularly macromolecules like plasmid DNA across skin, either by removing the stratum corneum through tape-stripping or use of physical methods. However, owing to their invasive and cumbersome nature, expensive setups, and patient non-compliance, attention has now shifted to the use of a non-invasive class of molecules (i.e., chemical or peptide-based penetration enhancers). Additionally, the careful design of nanocarriers has also been crucial in achieving this task.

We rationalized that for efficient penetration of small or macromolecules across skin using enhancers, the enhancers should possess certain essential properties (e.g., safe to administer, nontoxic, highly efficient, should not compromise the stratum corneum in an irreversible manner, and should be compatible with the other ingredients of formulation). Additionally, to enhance the delivery of plasmid DNA as nanocomplexes, where a cationic agent and plasmid DNA are electrostatically bound together, it is important that the enhancer used should not hamper complexation and stability.

We have previously reported a secondary amphipathic peptide, Mgep9, as a skin-tissue- and cell-penetrating peptide that can efficiently deliver plasmid DNA to skin in the form of nanocomplexes following non-invasive topical administration.³⁰ However, further enhancement of the bioavailability of these nanocomplexes in skin is desirable to eventually attain improved therapeutic effects. In this study, we focused on the use of enhancers to improve nanocomplex-mediated delivery of plasmid DNA.

Recent reports emphasizing the feasibility of using penetration enhancers for improved cargo delivery to skin predict SLA-PP mixture as a safe and potent chemical enhancer to be applied on skin.⁹ Moreover, SPPs such as SPACE, TD-1, AT1002, and polyarginines, to name few, are now being largely explored for the enhancement effects owing to their safe and non-immunological nature. Another chemical penetration enhancer, silicone oil, although less explored in this regard, finds wide utility as a constituent of cosmeceutical formulations.

However, all of these enhancers have only been used to impart increased delivery of small molecules in skin.

Hence, we wanted to check if these enhancers can also maintain this efficient activity in synergy with naturally penetrating nanocomplexes and further improve plasmid DNA delivery in skin. From our results, we could infer that overall, chemical enhancers were more efficient in attaining this effect than the SPP class of enhancers. One probable explanation for this could be that chemical enhancers primarily interact with the more abundant lipid component of the skin and thereby allow entry of large number of nanocomplexes through this route only, whereas SPPs are known to primarily interact with the keratin protein of corneocytes and might lead to continuous phase alteration of nanocomplexes for entry into skin.¹⁶ This in turn can reduce their rate of migration, and hence, desired effects are not attained in same time period, leading to low transfection efficiency. Another possibility could be that the various physicochemical properties of these SPPs, such as charge and hydrophobicity, might interfere with the stability of the nanocomplexes, causing disruption of electrostatic interactions between peptide and plasmid DNA and reduction in expression. Moreover, we observed strong expression in primary keratinocytes (as shown in [Figure S3](#)) both in presence and absence of silicone oil using higher doses of plasmid DNA.

These enhancers are capable of interacting with either the lipid or protein component of skin to mediate their activity. Hence, it is possible that they enter skin and affect its metabolic milieu. Therefore, we analyzed their effect on the activity of most abundant protease enzymes in skin. It was seen that SPPs and silicone oil did not hamper enzymatic activity in skin, unlike SLA-PP, which is a surfactant and has protein-denaturing tendency and exhibited decreased protease activity in skin. Since silicone oil was found to be both efficient and safe to use, we further analyzed possible toxicity to skin cells and tissue on application of silicone oil.

It was observed that use of this enhancer did not alter the cellular differentiation or skin tissue architecture or hamper cell viability *in vitro* or *ex vivo*. No necrosis of cells was observed in human skin tissue treated with this enhancer, and >80% cell viability was maintained in HaCaT cells and primary human keratinocytes, unlike SLA-PP, where significant cell death was recorded. Negligible permeation of skin-impermeable dyes on co-administration with silicone oil indicated that whatever changes in skin permeability take place are mild and transient. This is an advantage, as it reduces the risk of skin getting exposed to harmful allergens as well as pathogens subsequently. However, when we tried to locate the presence of FITC in skin tissue itself, we observed that in the case of silicone oil, no fluorescence was present, even in the skin section. This was an interesting observation, as it is expected that silicone oil, which is an enhancer, should improve the entry of FITC molecules. One possible reason could be that because it is hydrophobic in nature, the FITC molecule gets trapped in the silicone oil and is unable to go through. Alternatively, it may undergo rapid exocytosis across the skin, thus leading to the absence of any detectable signal. Therefore, the compatibility of

the physicochemical properties of enhancer and molecules delivered plays a crucial role in determining the enhancement efficiency. This also raises the question of whether the silicone oil itself is moving into the deeper layers of skin. This issue is discussed later.

After evaluating the safety potential of silicone oil, we then tried to understand the underlying mechanism by which it mediated its action in skin. Skin has three major pathways for the entry of molecules: (1) an intercellular pathway through the lipids, (2) a trans-cellular pathway through the cells, and (3) follicular or shunt pathways, which are minor contributors. We used the hairless mouse model for our *in vivo* studies. It is a well-established mouse model that lacks follicular opening and is thereby a better mimic of human skin than other known mouse models.^{36,37} The entry of nanocomplexes is primarily through non-follicular pathways in this model that are otherwise difficult to breach. Since we observed similar enhancement effect of silicone oil in the *ex vivo* study of human skin and the *in vivo* study of the SKH-1 mouse, this indicates that the presence or absence of follicles and other shunt pathways in skin does not influence the efficiency of this enhancer. Moreover, synergistic application of enhancer and nanocomplexes did not cause any immunogenic reaction.

Further, we used FTIR spectroscopy to understand the mechanism of action of silicone oil. We tried to address two questions: (1) whether treatment with silicone oil and nanocomplexes causes any major changes in the skin structure on topical application and (2) whether silicone oil is also directly entering skin. Our data indicate a possible alteration of skin hydration status that could be a contributing factor for the enhancement observed. Such changes in skin hydration can possibly disrupt the microstructure of skin, leading to swelling of corneocytes and creating intercorneocyte gaps and opening of porous aqueous pathways of skin by breaking desmosome junctions. We also observe mild fluidization of skin lipids from the FTIR spectrum, which indicates transient disturbance in the lipid assembly.^{38–40} Hence, overall permeability across skin is enhanced. Still, overall spectra of treated skin resembled that of the control skin, with no major distortions or shifting of peaks, indicating that silicone oil is safe to use as an enhancer. Moreover, the absence of silicone oil peaks in eluted fraction of solvent from viable epidermis seems to indicate the impermeability of the enhancer itself to enter skin in spite of its ability to mildly disturb skin lipids, making it a safe topical agent that remains on skin surface while the cargo gets into the epidermis efficiently. While the absence of penetration of silicone oil itself indicates its possible occlusive effects, this needs to be further supplemented with validations from other techniques.

In conclusion, our study reports silicone oil as a safe and efficient enhancer for effective increase of the bioavailability of nanocomplexes in skin. Mechanistic insights reveal occlusion effect of silicone oil on skin, which in turn alters the hydration status leading to possible opening of many porous channels that can mediate efficient movement of hydrophilic molecules into skin. Additionally high positive charge of the nanocomplexes further aids in their efficient entry across the skin. Thus it can assist these nanocomplexes in overcoming

the stratum corneum barrier of skin without compromising the tissue architecture and integrity aspects. The strategy paves an efficient way to realize the clinical translational potential of nucleic acid delivery in skin with improved bio-availability characteristics.

MATERIALS AND METHODS

Chemicals and Cell Lines

The peptides used in this study (Mgpe9 and TD-1) were custom synthesized (>98% purity) by Beijing SBS Genetech. Silicone oil laboratory reagents (LR) used was purchased from SD-Fine Chemicals Limited, with the specifications weight per milliliter at 20°C of ~0.970 g, kinetic viscosity ~300 cS, and recommended temperature stability 250°C. Chemical enhancer mixture (i.e., SLA-PP) were obtained from Sigma-Aldrich. Nanocomplexes were prepared using plasmid pEGFP-C1 (4.7 kb) or pMIR (6.4 kb) (Clontech Laboratories) that was amplified in *Escherichia coli* DH5 α strain and isolated using GenElute HP Endotoxin-Free Plasmid MaxiPrep kit (Sigma). All the chemicals and culture media used were also obtained from Sigma unless mentioned otherwise. A CellTiter Glo viability assay kit was purchased from Promega. HaCaT, which is an adult keratinocyte cell line, was a gift from Dr. Sudhir Krishna (The National Center for Biological Sciences [NCBS], Bangalore, India). Primary human keratinocytes were obtained from Lonza.

Preparation of Nanocomplexes

Nanocomplexes were prepared at N/P ratios (Z (+/-)) of 10, where N/P is defined as the ratio between total number of amines of a peptide and the total number of phosphates of a plasmid DNA. The preparation was carried out by gradual addition of 10 μ L plasmid DNA (20 ng/ μ L) for gel-based and cytotoxicity studies, 500 μ L plasmid DNA (40 ng/ μ L) for dynamic light scattering study, and 40 μ L plasmid DNA (100 ng/ μ L) for ex vivo and in vivo studies to 10 μ L, 500 μ L, or 40 μ L Mgpe9 peptide solution of appropriate concentration, respectively, in a drop-wise manner accompanied by constant vortexing. These nanocomplexes were then allowed to stabilize for 1 hr at room temperature before performing any experiment.

Dynamic Light Scattering

Briefly, 1 mL Mgpe9 nanocomplexes was prepared at Z = 10. The nanocomplexes were pretreated with enhancers (i.e., silicone oil, TD-1, and SLA-PP) for 30 min in independent setups, followed by estimation of mean hydrodynamic diameter using Zetasizer Nano ZS90 (Malvern Instruments) at 25°C. A minimum of three readings with replicates were recorded per sample. The untreated nanocomplexes were taken as experimental control.

DNA Condensation Assay

The electrophoretic mobility of the Mgpe9 nanocomplexes prepared at Z = 10 and pretreated with respective enhancers for 30 min (as mentioned before) was studied using agarose gel electrophoresis. 20 μ L nanocomplexes with 200 ng total DNA was loaded in each case onto 1% agarose gel containing ethidium bromide. Electrophoresis was carried out at 150 V in 1 \times TAE buffer (pH 7.4) for 45 min. The presence of free plasmid DNA was detected using

ethidium bromide fluorescence as seen through transilluminator (Bio-Rad ChemiDoc XRS+). Bare plasmid DNA was taken as experimental control.

Human Skin Tissue Pre-processing for Ex Vivo Studies

Human foreskin tissue (discarded sample collected in studies approved by the institutional human ethics committee [approval number IGIB/HEC/09/13]) obtained in transportation media (Hank's balanced salt solution [HBSS], Invitrogen) was washed three times alternatively with 1 \times PBS and 70% alcohol solution to clear contamination, if any. It was then processed into 0.5 cm \times 0.5 cm pieces using sterile scalpel and plated in small inserts (to cover the base area completely and avoid contamination from the edges owing to movement during treatment) in a 24-trans-well plate with 300 μ L keratinocyte-serum-free medium (K-SFM; Invitrogen) in the outer well such that only the dermis remained submerged in media whereas epidermis was exposed for the topical treatment. The plated tissue pieces were incubated at 37°C and monitored over a period of 24 hr to check for tissue quality and contaminations before proceeding with the experiments.

Plasmid DNA Delivery in Human Foreskin Tissue in the Presence of Enhancers

80 μ L Mgpe9 nanocomplexes was prepared at Z = 10 using EGFP-C1 plasmid (100 ng/ μ L) as described above. After 24 hr of skin tissue pre-processing, the tissue was pretreated for 30 min with SPP (TD-1) or chemical-based enhancers (SLA-PP or silicone oil) followed by topical administration of nanocomplexes in each well in independent experiments. The treatment with nanocomplexes in absence of any enhancer was considered as experimental control. This treatment was repeated for 3 days consecutively with a single such application per day (4 μ g plasmid DNA per application) along with intermittent washing of the tissue using 1 \times PBS before each of the fresh applications. 24 hr after the final application, the tissue was again washed in similar manner, fixed using 4% paraformaldehyde for 30 min at room temperature, transferred to 20% sucrose solution containing 0.01% sodium azide, and stored at 4°C until further processing. For cryosectioning (24 hr post-fixation), the tissue was embedded in an OCT compound, and sections of 6 μ m thickness were obtained and visualized for the presence of EGFP using immunostaining (as explained later). Untreated skin tissue was taken as technical control to avoid spurious results due to auto-fluorescence artifact.

Immunostaining Study to Locate the Presence of EGFP

Full-thickness human foreskin tissue was processed, plated, and treated topically as described above. Post-treatment tissue cryosections were obtained in a manner similar to that mentioned before and rehydrated using wash buffer (1 \times PBS with 0.1% Triton X-100) for 15 min, followed by 1 hr of blocking in 5% BSA at room temperature. Primary antibody (anti-EGFP) was applied to the tissues at dilution of 1:200 and incubated overnight at 2°C–8°C. The tissues were then given three washes of 15 min each in wash buffer before addition of tetramethyl rhodamine iso thio cyanate (TRITC)-labeled secondary antibody, anti-rabbit immunoglobulin G (IgG) against

EGFP at dilution of 1:250 for 1 hr at room temperature. The washing was repeated along with the final rinse using $1 \times$ PBS. The mounting of tissues was done with DAPI-antifade reagent (Invitrogen), and results were recorded using confocal microscopy (TCS SP8 confocal microscope, Leica Microsystems).

Flow Cytometry to Quantify EGFP in Skin

For quantification of EGFP fluorescence in the epidermis, the epidermis was removed from full-thickness skin tissue using overnight Dispase (0.25%) treatment at 4°C followed by incubation of the epidermis with 200 μL trypsin (0.25%) solution for 20 min at 37°C to allow cell separation to occur. The dissociated cells obtained were suspended in ice-cold $1 \times$ PBS and centrifuged at a speed of 2,000 rpm for 5 min at 4°C . After centrifugation, the pellet obtained was again washed using 500 μL ice-cold $1 \times$ PBS in similar manner followed by its resuspension in 200 μL $1 \times$ PBS for further analysis. The flow cytometry measurements were then performed using FACS Caliber (Becton Dickinson) to quantify the cellular fluorescence and mean fluorescence intensity. Statistical significance for quantitative data obtained was calculated using a two-tailed Student's *t* test (unpaired) in GraphPad Prism.

Plasmid DNA Delivery in Human Primary Keratinocytes and Cytotoxicity Analysis

Human primary keratinocytes were seeded at density of 50,000 cells/well in a six-well plate format using specific culture medium prescribed by Lonza. After 24 hr of plate preparation, 200 μL nanocomplexes, formed using Mgpe9 and 10 μg plasmid DNA encoding for EGFP, was added to each well (in the presence and absence of enhancers), after which the plate was incubated at 37°C . EGFP expression was then visualized 48 hr post-transfection, after removal of medium and washing the cells twice with $1 \times$ HBSS, using an inverted DMI6000B fluorescence microscope (Biomedical Research, Leica Microsystems). DAPI was used for nuclear staining of viable cells. Cell viability was also performed under similar conditions using CellTiter GLO method according to manufacturer's protocol.

Assessment of Skin Tissue Architecture

Full-thickness human foreskin tissue was processed, plated, and pretreated with silicone oil; SLA-PP for 30 min in independent experiments followed by topical treatment with nanocomplexes as mentioned before. Tissue treated with nanocomplexes in the absence of chemical enhancer and untreated skin tissue was used as experimental controls. The cryosections obtained after treatment were then examined in the microscope at $40\times$ to identify possible detachment of stratum corneum from viable epidermis or complete loss of stratum corneum. Moreover, cellular differentiation and identification of the skin layers was carried out in the cryosections by observing the presence of keratin 10 (Alexa-488-tagged anti-rabbit secondary antibody), loricrin (Alexa-Fluor-647-tagged anti-rabbit secondary antibody), and keratin 14 (Alexa-88-tagged anti-mouse secondary antibody) protein (a biochemical marker for this layer) using the immunostaining method as described in previous sections. Untreated skin tissue was taken as control for the latter study.

Skin Integrity Test

To check the effect of chemical enhancer and nanocomplexes on skin integrity, a skin permeability test was performed using equilibrated full-thickness human foreskin tissue pre-soaked for 24 hr in $1 \times$ PBS solution before conducting the study. 80 μL Mgpe9 nanocomplexes following pre-treatment of skin with silicone oil or SLA-PP as described before was added to the donor compartment along with 100 μL 2 $\mu\text{g}/\mu\text{L}$ FITC (389 Da) solution and 100 μL 1 mM dextran (3,000 Da) in independent experiments in all the setups. The system was kept under constant agitation at 250 rpm at room temperature, and 1 mL sample volume was collected at different time intervals (i.e., 0 hr or time of application, 1 hr, 2 hr, 3 hr, 4 hr, 5 hr, 18 hr, and 24 hr). The volume of receptor compartment was maintained constant by re-addition of 1 mL $1 \times$ PBS as a replacement. Untreated skin tissue was considered as experimental control. FITC fluorescence was recorded in the collected samples at emission wavelength of 525 nm using a microplate reader (Infinite 200 Pro, Tecan). Dextran was assessed by anthrone test for carbohydrates.

Protease Activity Assay

Briefly, skin tissue was treated with chemical penetration enhancers (silicone oil and SLA-PP) before application of Mgpe9 nanocomplexes, after which it was homogenized in liquid nitrogen using a mortar and pestle, and the powder tissue obtained was lysed using 500 μL RIPA buffer. Enzyme activity was assessed in the obtained tissue lysate using casein as substrate according to the standard bicinchoninic acid assay (BCA) protocol (Pierce). Tyrosine (1 mg/mL) was used to plot the standard curve. Protease activity obtained from untreated skin tissue was plotted as 100%, and relative activity was assessed.

Tissue Toxicity Assessment for Necrosis

Skin tissue was plated, treated, and processed in similar manner as mentioned before. Cryosections were washed three times using 500 μL PBS ($1 \times$) and 0.1% Triton X-100. Following this, it was stained using 10 μL propidium iodide solution (0.1 $\mu\text{g}/\mu\text{L}$) in 100 μL $1 \times$ PBS for 10 min at room temperature. After which the three washings were repeated using 500 μL PBS ($1 \times$) and red fluorescence was visualized using TCS SP8 confocal microscope (Leica). Untreated tissue and treatment without enhancers were taken as experimental controls.

Cell Viability Assay

HaCaT cells were seeded in a 96-well plate at density of 5,000 cells per well. After 24 hr, when 70% confluency was attained, complete media was replaced with 80 μL Opti-MEM (Invitrogen) in each well. Following this, 20 μL nanocomplexes (with final DNA concentration of 200 ng/well) in the presence and absence of the chemical enhancers silicone oil and SLA-PP was added to the cells. Cells were pre-exposed to enhancers for 30 min before the addition of Opti-MEM to each well followed by nanocomplex treatments. Cell viability was analyzed after 4 hr and 24 hr of incubation at 37°C (in the latter case, media was replaced with complete media after 4 hr) according to the manufacturer's protocol. Measurements were recorded in triplicate with three

measurements in each case using a microplate reader (Infinite 200 Pro, Tecan) and plotted as percentage cell viability.

Mechanism of Penetration Enhancement in Skin Using FTIR

In skin, stratum corneum was obtained by standard heat separation method. Stratum corneum membrane samples were cut into 0.5 cm × 0.5 cm pieces, and FTIR spectra was recorded on the skin tissue sample after pretreatment with silicone oil with Mgpe9 nanocomplexes for 24 hr. Untreated skin tissue was taken as experimental control. Spectra was obtained using the Thermo Scientific model NICOLET 380 FTIR operating in the range of 400–4,000 cm^{-1} with a resolution of 4 cm^{-1} and averaged over 400 scans.

In elute solution, skin tissue was treated with silicone oil only and silicone oil with Mgpe9 nanocomplexes to mimic three consecutive applications in independent experiments. Following this, stratum corneum was tape-stripped 20 times and silicone oil eluted from the viable epidermis tissue using a chloroform/acetone (1:1 v/v) mixture. The mixture obtained was scanned for FTIR spectra using the Thermo Scientific model NICOLET 380 FTIR operating in the range of 400–4,000 cm^{-1} with a resolution of 4 cm^{-1} . Spectra for bare silicone oil (taken as control for the study) were also recorded to identify signature peaks.

FITC Labeling of Plasmid DNA

pDNA (pEGFP-C1) was labeled with FITC using the Label IT Tracker Fluorescein kit (Mirus Bio) at a ratio of 0.75:1 (v/w) (i.e., 0.75 μL labeling reagent per microgram pDNA) according to the manufacturer's protocol.

Tissue Uptake of FITC-Labeled Complexes

Nanocomplexes were formed using FITC-labeled plasmid DNA, and skin tissue was topically treated with Mgpe9 nanocomplexes in the presence and absence of silicone oil as described in previous sections. Treatments were performed in a manner similar to that explained before, followed by washing, fixation, and cryosectioning of treated tissues. Presence of FITC-labeled nanocomplexes in skin was detected using confocal microscopy (TCS SP8, Leica Microsystems), and quantification of complexes in epidermis was done using flow cytometry analysis (BD FACS).

In Vivo Transfection Study

Entire animal studies were performed using 2- to 4-week-old hairless mice SKH-1 (irrespective of gender), and animal usage was in line with the approval by the institutional animal ethics committee (approval number IITR/IAEC/47/13). Each study was done in two groups, where each group comprised three mice ($n = 6$). In one of the groups, mice were pretreated topically with the chemical enhancer (silicone oil), whereas in other group, mice were kept untreated to serve as experimental controls. This was followed by topical administration of 80 μL Mgpe9 nanocomplexes prepared at charge ratio 10 in both groups. Treatment was continued for three consecutive days with a single application per day, where 4 μg plasmid DNA was administered per application on the dorsal surface of mice. This

was added into a circular plastic well (diameter = 1 cm) pre-adhered to skin and covering area of 3.14 cm^2 , and intermittent washing of skin surface was performed before each fresh application using 1 × PBS. The mice were sacrificed 24 hr after the final application, and skin tissue was obtained. Following this, the tissue was washed, fixed, cryosectioned, and processed for immunostaining in a manner similar to that explained previously for the ex vivo study.

Flow Cytometry to Quantify EGFP in SKH-1

SKH-1 was treated with 80 μL nanocomplexes as explained above, after which mice were sacrificed and skin tissue from the treated area was excised. For quantification of EGFP fluorescence in the skin, a single-cell suspension in 1 × PBS was obtained using a GentleMacs dissociator. The dissociated cells obtained were suspended in ice-cold 1 × PBS and centrifuged at a speed of 2,000 rpm for 5 min at 4°C. After centrifugation, the pellet obtained was again washed using 500 μL ice-cold 1 × PBS in a similar manner, followed by resuspension in 200 μL 1 × PBS for further analysis. Flow cytometry measurements were then performed using FACS Caliber (Becton Dickinson) to quantify cellular fluorescence and mean fluorescence intensity.

Luciferase Activity Estimation in SKH-1

SKH-1 was topically treated with 80 μL nanocomplexes formed using Mgpe9 peptide and pMIR luciferase plasmid as explained before at different sites within the same animal. 24 hr after the third application, mice were sacrificed and skin tissue from treated areas was excised. The skin tissue obtained was snap-frozen using liquid nitrogen in a mortar and lysed by the addition of cell culture lysis reagent (CCLR) using a pestle. The lysate obtained was then assessed for luciferase activity using the standard protocol from Promega and normalized, with total protein concentration estimated using the BCA method. Values were obtained and plotted as relative light units (RLU) \pm SD.

In Vivo Estimation of Inflammatory Cytokines

SKH-1 was topically treated with nanocomplexes and enhancers in similar manner as explained before, after which mice were sacrificed and 1.5 mL blood was collected in vacutainers. The samples were then allowed to stand at room temperature for 1 hr for serum separation. After 1 hr, samples were centrifuged at 1,500 rpm for 15 min for better separation. Serum samples collected were then analyzed for the presence of inflammatory cytokines, IL-2, IL-6, IL-12, and TNF- α using standard ELISA kits (eBioscience). SLA-PP was taken as positive control for the study. The concentrations were obtained and plotted as mean \pm SD.

SUPPLEMENTAL INFORMATION

Supplemental Information includes eight figures and can be found with this article online at <http://dx.doi.org/10.1016/j.ymthe.2017.03.009>.

AUTHOR CONTRIBUTIONS

M.G. and V.T.N. conceived and designed the experiments. M.G. wrote the manuscript. M.V. planned and performed experiments and assisted in writing of the manuscript. S.A. and K.M.A. contributed to the animal studies. N.G. and D.S. helped with FTIR

experiments. V.G. and H.G. assisted with primary keratinocytes and skin tissue studies.

CONFLICTS OF INTEREST

The authors declare no conflict of interest.

ACKNOWLEDGMENTS

We acknowledge the Council of Scientific and Industrial Research (CSIR), New Delhi, India (Network Project TOUCH: BSC0302) for providing financial support. We also thank Aanchal Gupta (CSIR-IGIB), Balaram Ghosh (CSIR-IGIB), and Bijay Ranjan Pattnaik (CSIR-IGIB) for experimental support. We also acknowledge Manish Kumar (CSIR-IGIB) and funding from BSC0403 for the confocal studies.

REFERENCES

1. Prausnitz, M.R., and Langer, R. (2008). Transdermal drug delivery. *Nat. Biotechnol.* 26, 1261–1268.
2. Prausnitz, M.R., Mitragotri, S., and Langer, R. (2004). Current status and future potential of transdermal drug delivery. *Nat. Rev. Drug Discov.* 3, 115–124.
3. Paudel, K.S., Milewski, M., Swadley, C.L., Brogden, N.K., Ghosh, P., and Stinchcomb, A.L. (2010). Challenges and opportunities in dermal/transdermal delivery. *Ther. Deliv.* 1, 109–131.
4. Naik, A., Kalia, Y.N., and Guy, R.H. (2000). Transdermal drug delivery: overcoming the skin's barrier function. *Pharm. Sci. Technol. Today* 3, 318–326.
5. Barua, S., and Mitragotri, S. (2014). Challenges associated with penetration of nanoparticles across cell and tissue barriers: a review of current status and future prospects. *Nano Today* 9, 223–243.
6. Mitragotri, S. (2005). Immunization without needles. *Nat. Rev. Immunol.* 5, 905–916.
7. Desai, P., Patlolla, R.R., and Singh, M. (2010). Interaction of nanoparticles and cell-penetrating peptides with skin for transdermal drug delivery. *Mol. Membr. Biol.* 27, 247–259.
8. Bos, J.D., and Meinardi, M.M. (2000). The 500 Dalton rule for the skin penetration of chemical compounds and drugs. *Exp. Dermatol.* 9, 165–169.
9. Karande, P., Jain, A., and Mitragotri, S. (2004). Discovery of transdermal penetration enhancers by high-throughput screening. *Nat. Biotechnol.* 22, 192–197.
10. Karande, P., Jain, A., Ergun, K., Kispersky, V., and Mitragotri, S. (2005). Design principles of chemical penetration enhancers for transdermal drug delivery. *Proc. Natl. Acad. Sci. USA* 102, 4688–4693.
11. Williams, A.C., and Barry, B.W. (2004). Penetration enhancers. *Adv. Drug Deliv. Rev.* 56, 603–618.
12. Guy, R.H., Kalia, Y.N., Delgado-Charro, M.B., Merino, V., López, A., and Marro, D. (2000). Iontophoresis: electrorepulsion and electroosmosis. *J. Control. Release* 64, 129–132.
13. Mitragotri, S., Blankschtein, D., and Langer, R. (1995). Ultrasound-mediated transdermal protein delivery. *Science* 269, 850–853.
14. Finnin, B.C., and Morgan, T.M. (1999). Transdermal penetration enhancers: applications, limitations, and potential. *J. Pharm. Sci.* 88, 955–958.
15. Elsayed, M.M., Abdallah, O.Y., Naggar, V.F., and Khalafallah, N.M. (2007). Lipid vesicles for skin delivery of drugs: reviewing three decades of research. *Int. J. Pharm.* 332, 1–16.
16. Kumar, S., Zakrewsky, M., Chen, M., Menegatti, S., Muraski, J.A., and Mitragotri, S. (2015). Peptides as skin penetration enhancers: mechanisms of action. *J. Control. Release* 199, 168–178.
17. Aliyar, H., and Schalaus, G., 2nd (2015). Recent developments in silicones for topical and transdermal drug delivery. *Ther. Deliv.* 6, 827–839.
18. Montenegro, L., Paolino, D., and Puglisi, G. (2004). Effects of silicone emulsifiers on *in vitro* skin permeation of sunscreens from cosmetic emulsions. *J. Cosmet. Sci.* 55, 509–518.
19. Puri, N., and Talwar, A. (2009). The efficacy of silicone gel for the treatment of hypertrophic scars and keloids. *J. Cutan. Aesthet. Surg.* 2, 104–106.
20. Blasdale, B., Finnegan, S., Murray, K., Kelly, S., and Percival, S.L. (2015). The use of silicone adhesives for scar reduction. *Adv. Wound Care (New Rochelle)* 4, 422–430.
21. Hsu, T., and Mitragotri, S. (2011). Delivery of siRNA and other macromolecules into skin and cells using a peptide enhancer. *Proc. Natl. Acad. Sci. USA* 108, 15816–15821.
22. Rothbard, J.B., Garlington, S., Lin, Q., Kirschberg, T., Kreider, E., McGrane, P.L., Wender, P.A., and Khavari, P.A. (2000). Conjugation of arginine oligomers to cyclosporin A facilitates topical delivery and inhibition of inflammation. *Nat. Med.* 6, 1253–1257.
23. Chen, Y., Shen, Y., Guo, X., Zhang, C., Yang, W., Ma, M., Liu, S., Zhang, M., and Wen, L.P. (2006). Transdermal protein delivery by a coadministered peptide identified via phage display. *Nat. Biotechnol.* 24, 455–460.
24. Uchida, T., Kanazawa, T., Takashima, Y., and Okada, H. (2011). Development of an efficient transdermal delivery system of small interfering RNA using functional peptides, Tat and AT-1002. *Chem. Pharm. Bull. (Tokyo)* 59, 196–201.
25. Hou, Y.W., Chan, M.H., Hsu, H.R., Liu, B.R., Chen, C.P., Chen, H.H., and Lee, H.J. (2007). Transdermal delivery of proteins mediated by non-covalently associated arginine-rich intracellular delivery peptides. *Exp. Dermatol.* 16, 999–1006.
26. Kim, Y.C., Ludovice, P.J., and Prausnitz, M.R. (2007). Transdermal delivery enhanced by magainin pore-forming peptide. *J. Control. Release* 122, 375–383.
27. Chen, M., Gupta, V., Anselmo, A.C., Muraski, J.A., and Mitragotri, S. (2014). Topical delivery of hyaluronic acid into skin using SPACE-peptide carriers. *J. Control. Release* 173, 67–74.
28. Lee, J., Jung, E., Park, J., and Park, D. (2005). Transdermal delivery of interferon-gamma (IFN-gamma) mediated by penetratin, a cell-permeable peptide. *Biotechnol. Appl. Biochem.* 42, 169–173.
29. Chen, M., Kumar, S., Anselmo, A.C., Gupta, V., Slee, D.H., Muraski, J.A., and Mitragotri, S. (2015). Topical delivery of Cyclosporine A into the skin using SPACE-peptide. *J. Control. Release* 199, 190–197.
30. Vij, M., Natarajan, P., Pattnaik, B.R., Alam, S., Gupta, N., Santhiya, D., Sharma, R., Singh, A., Ansari, K.M., Gokhale, R.S., et al. (2016). Non-invasive topical delivery of plasmid DNA to the skin using a peptide carrier. *J. Control. Release* 222, 159–168.
31. Panchaxari, D.M., Pampana, S., Pal, T., Devabhaktuni, B., and Aravapalli, A.K. (2013). Design and characterization of diclofenac diethylamine transdermal patch using silicone and acrylic adhesives combination. *Daru* 21, 6.
32. Smith, A.L., Winefordner, J.D., and Kolthoff, I.M. (1991). *The Analytical Chemistry of Silicones* (John Wiley & Sons, Inc), pp. 210–211.
33. Reusch, W. (2013) *Introduction to spectroscopy*. <https://www2.chemistry.msu.edu/faculty/reusch/virttxtjml/Spectrpy/spectro.htm#contnt>.
34. Barry, B.W., Edwards, H.G.M., and Williams, A.C. (1992). Fourier transform raman and infrared vibrational study of human skin: assignment of spectral bands. *J. Raman Spectrosc.* 23, 641–645.
35. Clancy, M.J., Corish, J., and Corrigan, O.I. (1994). Comparison of the effects of electrical current and penetration enhancers on the properties of human skin using spectroscopic (FTIR) and calorimetric (DSC) methods. *Int. J. Pharm.* 105, 47–56.
36. Benavides, F., Oberszyn, T.M., VanBuskirk, A.M., Reeve, V.E., and Kusewitt, D.F. (2009). The hairless mouse in skin research. *J. Dermatol. Sci.* 53, 10–18.
37. Honzak, L., Sentjurc, M., and Swartz, H.M. (2000). *In vivo* EPR of topical delivery of a hydrophilic substance encapsulated in multilamellar liposomes applied to the skin of hairless and normal mice. *J. Control. Release* 66, 221–228.
38. Tan, G., Xu, P., Lawson, L.B., He, J., Freytag, L.C., Clements, J.D., and John, V.T. (2010). Hydration effects on skin microstructure as probed by high-resolution cryo-scanning electron microscopy and mechanistic implications to enhanced transcutaneous delivery of biomacromolecules. *J. Pharm. Sci.* 99, 730–740.
39. Prausnitz, M.R., Elias, P.M., Franz, T.J., Schmuth, M., Tsai, J.C., Menon, G.K., Holleran, W.M., and Feingold, K.R. (2012). Skin Barrier and Transdermal Drug Delivery (Medical Therapy).
40. Warner, R.R., Stone, K.J., and Boissy, Y.L. (2003). Hydration disrupts human stratum corneum ultrastructure. *J. Invest. Dermatol.* 120, 275–284.